IEEE Access
Multidisciplinary ⋮ Rapid Review ⋮ Open Access Journal

Received November 10, 2020, accepted November 29, 2020, date of publication December 9, 2020,
date of current version December 21, 2020.

Digital Object Identifier 10.1109/ACCESS.2020.3043528

Center-Symmetrical Object Detection Based on Gabor Wavelets

YI ZHANG[1], (Member, IEEE), MIN ZOU[1], MENGBO YOU[2], (Member, IEEE), AND TAKUYA AKASHI[3], (Member, IEEE)

[1]Graduate School of Engineering, Iwate University, Morioka 020-8551, Japan
[2]College of Information Engineering, Northwest A&F University, Yangling 712100, China
[3]Faculty of Science and Engineering, Iwate University, Morioka 020-8551, Japan

Corresponding author: Takuya Akashi (akashi@iwate-u.ac.jp)

ABSTRACT Symmetry is an important visual characteristic in the image and can be used to identify real-world objects based on their geometrically balanced structures. Although image analysis of axisymmetry has been studied for years and many approaches have been developed to detect axisymmetry, image analysis of center-symmetry has been received little attention. Symmetrical center detection is a very important inspection for image analysis. The detected result is useful for image processing, such as object detection, image inpainting. It is difficult to detect the symmetrical center for the real-world image. Because the symmetrical objects usually appear some geometric transformation making them not perfectly center-symmetrical. This article proposes a novel weight voting approach to detect the global symmetrical center from a single image, noted as weight voting for center-symmetrical object detection (WVCS). Firstly, we sampled some feature points to vote for the global symmetrical center. Then, the orientation of Log-Gabor response and color information of HSV space are utilized as the feature descriptor to compute a similarity measure for two points. A proposed penalty term is employed to focus on the center-symmetrical objects in the foreground. The position with the maximal weight voted by all sampled feature points represents the symmetrical center. Based on the detected symmetrical object can be detected by fitting the symmetrical feature point pairs. The experimental results show that the WVCS outperforms other state-of-the-art algorithms while detecting the symmetrical center and objects from real-world images.

INDEX TERMS Gabor wavelets, symmetrical center detection, center-symmetrical object, similarity measure.

I. INTRODUCTION

Symmetry is one of the important visual properties for humans and organisms in general. In computer vision, it is also a very important property for object detection, segmentation, image inpainting, etc. Nowadays, reflection symmetry has been attracted much attention, and there are several state-of-the-art methods [1]–[6]. However, there is a type of symmetrical objects sharing the same characteristic in appearance, which is not always axisymmetrical but centrosymmetric. For instance, parallelogram objects are not axisymmetrical but centrosymmetric. Circular objects normally have many axial symmetries but only one symmetrical center. The position of the single symmetrical center can describe its geometrical structure better than any axial symmetries. However, there is very little research on using center-symmetry to detect objects, while including the symmetrical parts of objects, regions, scenes.

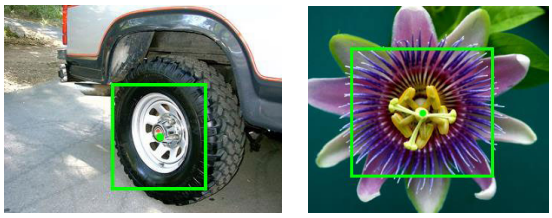

(a) (b)

FIGURE 1. Example of center-symmetrical object detection. (a) Wheel. The center-symmetrical object has the out-of-plane transformation. (b) Flower, an approximately center-symmetrical object. The proposed method can detect the symmetrical object and its center for both cases.

As shown in Fig. 1, some symmetrical objects are rotated along the out-of-plane direction and not strictly symmetrical in appearance while examining the image. The affine

The associate editor coordinating the review of this manuscript and approving it for publication was Byung-Gyu Kim.

transformation can only recover some in-plane rotation making the appearance of the object to be nearly symmetrical. However, the parameters of affine transformation need much computation to be optimized for an arbitrary image. As so far, existing approaches cannot extract the symmetry of objects in this case. Therefore, this article focus on detecting the center-symmetrical objects from images in real-world scenes by exploring the center of symmetry in the objects.

In recent years, a convolutional neural network (CNN) has been widely used for object detection, such as YOLOv3 [7], Fast R-CNN [8], and Mask R-CNN [9]. Deep learning methods can provide object detection proposals that contain symmetrical objects for image processing. However, the methods based on CNNs are still inappropriate to directly handle center-symmetrical object detection owing to the issues of limited segmentation accuracy and expensive manual annotation. In unconstrained environments, the practical requirements concerning higher detection accuracy and faster speed make the center-symmetrical object detection problem even more challenging.

In this article, we propose a center-symmetrical detection method based on the characteristic of center-symmetry with the symmetrical center. This method is noted as weight voting for center-symmetrical object detection (WVCS). The symmetrical center detection problem is difficult for real-world images due to the following reasons: 1) the target object sometimes does not show a perfectly center-symmetrical object appearance. 2) There is a large possibility that the background also has some center-symmetrical regions. 3) The target object may vary in size, shape, and position. To solve these problems, a weight voting method based on some discrete feature points is proposed, in which a similarity measure based on HSV color feature and local orientation is utilized to obtain the weight of patch pairs, owing to the good performance of these features in symmetrical object detection. Moreover, a penalty term is employed to suppress the influence of generic background parts and assign more weights to the center-symmetrical objects. As a result, our method can preferentially focus on center-symmetrical objects in the foreground. The experiments illustrate that our method can find the symmetrical center. Finally, the characteristic of center-symmetry is utilized to detect center-symmetrical objects.

To summarize, the main contribution of this article can be concluded as follows:

- We propose a robust symmetrical center detection approach for the image analysis of approximately center-symmetrical objects.
- A similarly measure method is proposed to obtain the weight of patch pairs.
- A penalty term is utilized to suppress the influence of background parts and assign more weights to the center-symmetrical objects.
- A dataset of center-symmetrical objects was collected from the *Seungkyu Lee dataset* [10], and labeled with center-symmetric objects and their centers.

II. RELATED WORKS

Symmetry detection researches have been attracted more and more attention in the last decade. Loy and Eklundh [11] proposed an efficient method for exploring symmetrical constellations of features in the images and presented the computation of symmetries in the image plane. The method uses three steps to perform the detection task. Firstly, the relevant local feature points are extracted using the response of SIFT [12]. Secondly, based on the SIFT descriptors, the pair-wise matching is computed. Finally, Hough-style voting space is used to determine the dominant symmetries present in the image.

Based on the method proposed by Loy [11], many researchers have proposed some improvements and refinements for this task. Mo and Draper [13] proposed the improvement that grouping sets of points are utilized instead of finding the closest matching to obtain the candidate bilateral symmetrical pairs of local patches. They also proposed to use the simple Hough-voting instead of complex vote weighted by orientation and scale. Moreover, there are some methods that the weight voting method is utilized to deal with some practical problems, such as face [14] and palmprint [15] recognition.

Edge information extraction with Log-Gabor [16] filter has been used in WVCS. Gabor [17] feature can also be used for simultaneously localizing spatial and frequency information. However, the normal Gabor filter has the weakness that even an asymmetrical filter will have a DC component and makes it difficult to extract symmetrical features. Therefore, the Log-Gabor filter computed with a logarithmic function is utilized. Besides, feature extraction based on Log-Gabor filter has been successfully used in different computer vision tasks, such as image enhancement [18], face recognition [19], image retrieval [20], and character segmentation [21].

Another important aspect is the similarity measure for obtaining the weight of patch pairs. Some pixel-wise methods like sum of absolute difference (SAD), sum of square difference (SSD), and normalized cross-correlation (NCC) [22], [23] are most widely used for similarly measure, due to their efficiency and simplicity. However, these methods are hard to deal with non-rigid transformations. For this problem and other noises in unconstrained environments, instead of pixel-wise local information, involving global information for designing a robust similarity descriptor is regarded as a key cue. Histogram similarly measure has been successfully applied to object detection and visual tracking tasks [24]–[26], and has the strength of robustness to geometric transformation. In this article, our similarity measure method is also motivated by the histogram, which is utilized the features of the orientation of Log-Gabor response and color information of HSV.

III. METHODOLOGY

A. PROBLEM DESCRIPTION

Our purpose is to find the center of the symmetrical object, noted as c. Motivated by the [13], [27], a weight voting

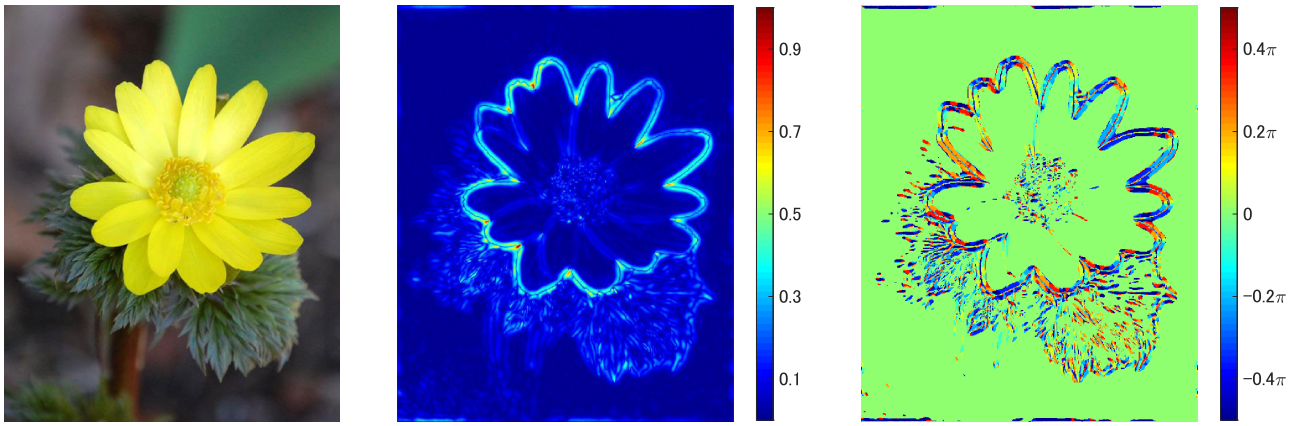

FIGURE 2. Log-Gabor response. (a) The original image. (b) The amplitude map, and the amplitude is normalized to [0,1]. (c) The orientation map $\theta \in [-\pi/2, \pi/2]$.

method is proposed to detect the symmetrical object. Instead of the Hough-voting for symmetrical axis, we proposed a simple weighted vote strategy for the symmetrical center c. We extract feature point f from the image to form a set F. Then, a similarity measurement $W(f_i, f_j)$ is proposed to measure the symmetrical for a pair of feature points. Each feature point pair (f_i, f_j) votes for its central region with weight $W(f_i, f_j)$. The weight map for each candidate position of the image can be obtained. Finally, symmetrical center detection can be described as follows:

$$(x_c, y_c) = arg\ max\ weightMap(x, y),$$
$$\text{s.t. } weightMap(x, y) = \sum_i \sum_j W(f_i, f_j). \quad (1)$$

Then, the symmetrical object can be detected by find the boundary that is center-symmetrical with (x_c, y_c).

B. FEATURE POINT EXTRACTION

We noticed that shape is an important indicator of whether a object is centrally symmetrical or not. Most shapes can be represented by their edges for further processing. We follow the idea in [27] to use the Log-Gabor filter to detect the edges of the target image. Then, around the edge, some feature points are extracted to vote for the object center. Different from [27], we not only use feature points of edges but also use another part of feature points that are extracted with the same space interval for center-symmetry analysis. That is to ensure that some flat or gradient objects can be detected. In this section, we will introduce the Log-Gabor based edge detection and the feature point extraction.

1) LOG-GABOR EDGE DETECTION

The Log-Gabor filter suppresses the negative effect of the DC component by logarithmic transformation of a Gabor filter in the Fourier domain. The Log-Gabor filter can be expressed by:

$$G_{s,o}(\rho, \theta) = exp\left(\frac{\left|atan\left(\frac{sin(\theta-\theta_0)}{cos(\theta-\theta_0)}\right)\right|}{2\sigma_\theta^2}\right) exp\left(\frac{-log\left(\frac{\rho}{\rho_0}\right)^2}{2log\left(\sigma_\rho\right)^2}\right) L(\rho) \quad (2)$$

where (ρ, θ) represent radial and angular in the Log-Gabor coordinates, (s, o) are the multiple scales and orientations respectively. Which over S scales and O orientations with their bandwidths $(\sigma_\rho, \sigma_\theta)$, which $s \in \{1, .., S\}$ and orientations $o \in \{\frac{z\pi}{O} | z = 0, .., O-1\}$. And (ρ_0, θ_0) are the frequency centers. A low-pass butterworth filter $L(\rho)$ is multiplied to the radial filter with order 15, and frequency 0.5, to eliminate any extra frequency at Fourier corners. The modulus of complex wavelet coefficients $I_{s,o}(x, y)$ are computed on the target image I as follows:

$$I_{s,o}(x, y) = \left|FT^{-1}\left(FT\left(g(I) \times G_{s,o}\right)\right)\right|, \quad (3)$$

where $g(\cdot)$ is function that utilized to obtained the the gray-scale version of target image I, and $FT(\cdot)$, $FT^{-1}(\cdot)$ are the Fourier transform and its inverse. Figure 2 illustrates an example of Log-Gabor response $I_{s,o}$ on a natural image with $S = 6$ and $O = 7$. The maximal amplitude in each pixels is shown Fig. 2(c), and corresponded orientation is shown in Fig. 2(e). Observably, the value of amplitude is extremely large around the edge. The value of orientation is similar in the symmetrical position of the object.

2) SAMPLING FEATURE POINTS

To deal with various targets, both spatial sampling points F^s and around edge feature points F^e are sampled in our work. Existing refection symmetry detection methods, such as [27], [28], only extract features F^e. In the normal case, these methods deal with the symmetry axis detection problem well. However, for color gradient objects, these methods do

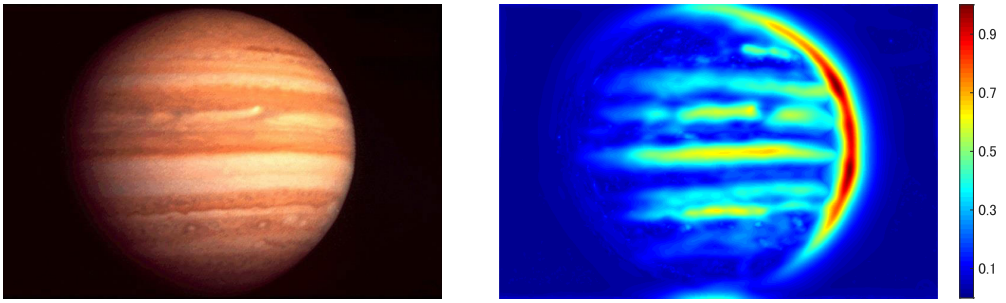

(a) Original (b) Amplitude

FIGURE 3. Amplitude of Log-Gabor image for gradient image. (a) Original image. (b) Amplitude image of (a). We can observe that the amplitude is small in left gradient part. Therefore, only using the edge part cannot detect the center-symmetrical object.

not perform well, which results from the obscure edges. As shown in Fig. 3, the left half edge of the object is obviously deficient. In our method, spatial sampling is integrated to edge feature extraction to deal with this problem. The detailed feature point sampling method is introduced as follows.

Firstly, the target images I is spatially sampled using non-interleaved patches along a regular grid. The stride and patch size are proportional to the maximum image dimension diagonal of I. This type of extracted feature points is F^s. Then, we extract another type of feature point set F^e for symmetrical center detecting. The $f_i^e \in F^e$ is the point which has maximal amplitude in $f_i^s \in F^s$, and the amplitude of f_i^e more than $kf_{\max}$, in which the $f_{\max}$ is the maximal amplitude of whole image, $k \in [0, 1]$ is a constant. k is employed to ensure f_i^e is included in edges.

C. FEATURE DESCRIPTOR

In WVCS, measuring the feature points pairs reasonably is important for symmetrical center voting. For point pair measurement, the core part is feature extraction. The textural and color information are prominent similarity characteristics for natural images, describing the symmetrical behavior of the balanced distribution of luminance and chrominance components, and local edge orientation. Hence, we introduce a statistical HSV-value histogram in patch J_i, which denotes the neighborhood patch around a feature point f_i with size $w \times w$. The local HSV histogram h^{HSV} is defined as following:

$$h_i^{HSV}(t_1, t_2, t_3) = \sum_{p \in J_i} \prod_{m=1}^{3} \delta\left(V_m(p), R(t_m)\right),$$
$$R(t_m) = \left[\frac{t_m - 1}{C_m}, \frac{t_m}{C_m}\right), \tag{4}$$

where $\delta(ele, set)$ is an indicator function when the element ele belong to the set return 1 else return 0. And $V_1(\cdot)$, $V_2(\cdot)$ and $V_3(\cdot)$ are the values in hue, saturation and value, respectively, in which the HSV values are normalized to $[0, 1]$. C_1, C_2, and C_3 are the numbers of bins for three color channels, and $t_1/t_2/t_3 \in \{1, 2, \ldots, C_1/C_2/C_3\}$ are the variables, which assist to define the range R of the channels.

Additionally, we use the orientation to measure the patch similarity. Only the color histogram is not adequate to measure the similarity between two patches. That result from some object maybe symmetrical in texture but not in color. Hence, the orientation is also integrated into the similarity measurement. As shown in Fig. 2(e), the orientations are always the same in symmetrical positions. A point p is extracted within patch J_i that is around $f_i \in F$ using the wavelet response of Log-Gabor filter $I_{s,o}(p^i)$, associated with its maximum wavelet response alongside with the corresponding orientation θ. We make the histogram h^o of orientation for the patch J_i.

$$h_i^o(n) = \sum_{p \in J_i} \delta(\theta(p), o_n), \; o_n = \left[\frac{(n-1)\pi}{N}, \frac{i\pi}{N}\right), \tag{5}$$

where N is the number of bin. The variable $n \in \{1, 2, \ldots, N\}$ is utilized to define the range o_n. And $\theta(p)$ is the orientation of the maximal magnitude that obtained by Log-Gabor response at feature point p. Histogram h^o is circularly shifted with respect to the orientation of the maximal magnitude among the neighborhood patch J_i.

D. SIMILARITY MEASURE FOR PATCH PAIR

In this article, the overlapped part of h_i^{HSV} and h_j^{HSV} is utilized to measure the color similarity of two patches f_i and f_j.

$$S^c(f_i, f_j) = \sum_{t_1=1}^{C_1} \sum_{t_2=1}^{C_2} \sum_{t_3=1}^{C_3} \frac{min\left(h_i^{HSV}(t_1, t_2, t_3), h_j^{HSV}(t_1, t_2, t_3)\right)}{h_a^{HSV}(t_1, t_2, t_3)}, \tag{6}$$

which $h_a^{HSV}(c)$ is the HSV histogram for whole image. We penalize the pixels that frequently appear by $h_a^{HSV}(c)$ that inspired by [29]. That result from the frequently appear pixels is more likely in the background. Figure 4 illustrates an example of color weight, that is utilized to penalize the frequently appear pixels.

In addition, the orientation is also utilized to measure the similarity of the patch pair. According to the center-symmetrical object characteristic, the 180° rotated object is

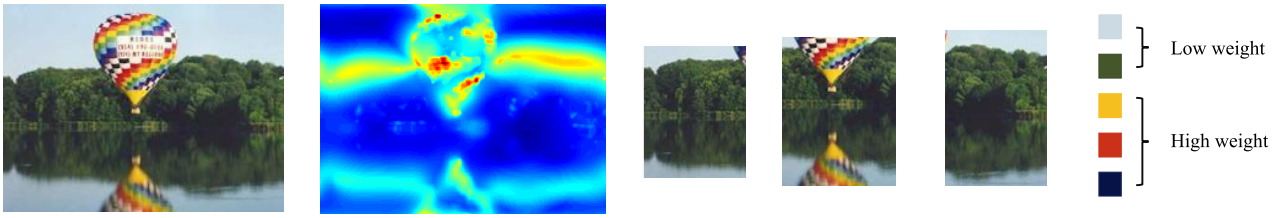

(a) Target image (b) Amplitude image (c) Candidate regions (d) Color weight

FIGURE 4. Color weight. (a) A target image. (b) The amplitude image of (a). (c) Three candidates are extracted from the regions of large amplitude. And it is difficult to distinguish which candidate is our target. (d) The examples of color weight.

the same as the original object and the orientations of corresponding symmetrical positions are also the same. Similar to the HSV histogram measure, we also use the overlapped parts to measure the similarity of two patches. The measuring function of orientation similarity is shown as follows:

$$S^o\left(f_i, f_j\right) = \sum_{n=1}^{N} min\left(h_i^o\left(n\right), h_j^o\left(n\right)\right). \tag{7}$$

With the defined $S_o(\cdot)$ and $S_c(\cdot)$, we can evaluate the weight of each patch pair and vote for the symmetrical center. There is a set of feature pairs by traversing f_i and f_j (i≠j). The size of the feature pairs set is $\frac{P(P-1)}{2}$, where P is the number of the feature point. The weight of pair (f_i, f_j) is calculated by the following formula:

$$W\left(f_i, f_j\right) = \frac{S^o\left(f_i, f_j\right) \times S^c\left(f_i, f_j\right)}{dis\left(f_i, f_j\right) + 1}, \tag{8}$$

where $dis(f_i, f_j)$ is the distance between f_i and f_j, and the distance is normalized to [0,1].

E. SYMMETRICAL CENTER VOTING

After the weight of patch pair $W\left(f_i, f_j\right)$ is computed, we can obtain the voting map by traversing each (f_i, f_j) as shown in:

$$weightMap\left(x, y\right) = \frac{1}{\sqrt{2\pi}\sigma} exp\left(-\frac{d^2}{2\sigma^2}\right) W\left(f_i, f_j\right), \tag{9}$$

which d is the distance between the midpoint of (f_i, f_j) and (x, y). And σ is set as the half of patch width $w/2$. Feature point pair (f_i, f_j) is any two elements selected from F, and $i \neq j$. The highest scoring point represents the symmetrical center (x_c, y_c).

F. SYMMETRICAL OBJECT FITTING

After the symmetrical center is detected, symmetrical object can be fitted by the center-symmetrical characteristic. The feature point pairs, whose midpoint are far away from the symmetrical center (x_c, y_c), are not needed to consider for symmetrical object detection. We have noticed that the weight of the feature point pair is very low in the background region, which results from the background penalty item. Moreover, the feature point pairs outside the symmetrical object are most likely asymmetrical. The object can be extracted by judging the edges from these differences. The center point (x_c, y_c) with diameter ϕ will form a circle. When the circle is contained in the object, in the Eq. 10 the $\sum W\left(f_i, f_j\right)/\phi$ will increase as ϕ increases. Because the number of symmetrical patch pair is positively correlated with ϕ^2. If the circle contains the entire object and some background, the $\sum W\left(f_i, f_j\right)/\phi$ will becomes smaller with ϕ increase, due to the increased patch pairs are in the background region, and these pairs are most likely asymmetrical. Consequently, our problem can be converted to maximizing the following equation:

$$\begin{aligned} \phi_m = arg\ max \sum W\left(f_i, f_j\right)/\phi, \\ \text{s.t. } dis\left(f_i, f_j\right) < \phi, dis\left(\left(x_c, y_c\right), ct\left(f_i, f_j\right)\right) < w/2, \end{aligned} \tag{10}$$

where $ct(\cdot)$ is the midpoint position. With ϕ_m determined, we can detect the object by the region inside the circle whose center is (x_c, y_c) and the diameter is ϕ_m. And the feature points that inside this circle form a point set F'. Finally, the minimal rectangle, in which all the feature points $f' \in \left(F^e \cap F'\right)$ are included, is our result.

IV. EXPERIMENT

In this section, we will introduce the detail of public symmetry datasets, evaluation metrics for performance comparison of the WVCS. Besides, some comparing methods are employed to show the superiority of our method.

A. IMPLEMENTATION

In this section, we will introduce the implementation details. The threshold of k is set as 0.2, which is utilized to select feature points. It is determined by experience. In the Log-Gabor filter, the orientations O and scales S are set as 32, 12, respectively. The numbers of the HSV's bin are set as 8, 2, 2 in hue, saturation, and value channel, respectively. And the width of patch w is one-fiftieth of a diagonal. The following experiments are all under these parameters.

B. DATASET DESCRIPTION

There is no currently available database for evaluating the problem of center-symmetrical object detection. Because our problem that searching for the symmetrical center is firstly proposed, we select from the reflection symmetrical detection datasets, *ICCV2017 training datasets: Seungkyu*

Lee datasets [10], this dataset contains reflection and rotation symmetry images, and it also contains center-symmetric objects in some of them. We selected center-symmetrical images and labeled them with center-symmetric objects and their centers. We extract 110 center-symmetrical images to construct a dataset for evaluating the symmetrical center detection problem. We also artificially annotate the ground truth for each image.

C. EVALUATION METRICS

The most important metric is the central deviation d_{rg}. Moreover, to evaluate the image of different size, $d_{ratio} = d_{rg}/diag$ is utilized to evaluate the performance. The *diag* is the diagonal of target image. Another metric is overlap rate *OR* that is also employed to measure the detected object for evaluating the performance.

$$OR = \frac{R_{obj} \cap G_{obj}}{R_{obj} \cup G_{obj}}, \tag{11}$$

in which R_{obj} is the detected object and G_{obj} is the ground truth.

D. COMPARISON METHODS

There are few methods for the symmetrical center detection problem before our work. Moreover, our dataset has many circular and eclipse objects. Therefore, circle detection method [30] and eclipse detection method [31] are utilized as the comparison method, noted as *circle* and *eclipse*, respectively. On the other hand, a very important factor in our method is the similarity measurement for patch pairs. The similarity measurement algorithms in [32] and [27] are utilized to illustrate the superiority of the WVCS. We note these two methods as histogram measure (HM) and ICCV2017, respectively.

E. RESULTS AND ANALYSIS

1) SYMMETRICAL CENTER

As shown in Fig. 5, the eclipse detection method [31] is stronger than circle detection [33] for the symmetrical center detection. However, these particular shape detection methods are worse than discrete voting methods, because of the limitations of object shape. The method of ICCV2017 performs better than the HM method, and the WVCS achieves the best performance.

Moreover, the visualization result is shown in Fig. 7. From Fig. 7(a), we can clearly observe that our method is superior to other comparison methods. We observed that only utilized histogram matching (HM) may treat the background as a symmetrical object, as shown in the first, second, fourth, and fifth row, results from the background has too much weight in its weight map. Although the method of ICCV2017 can deal with this problem by excluding flat areas, if the color gradient is low, this method fails as shown in the third row. Our approach can deal with these problems by introducing a background penalty item and the patches sampling algorithm. As shown in the sixth row, the WVCS also can deal with

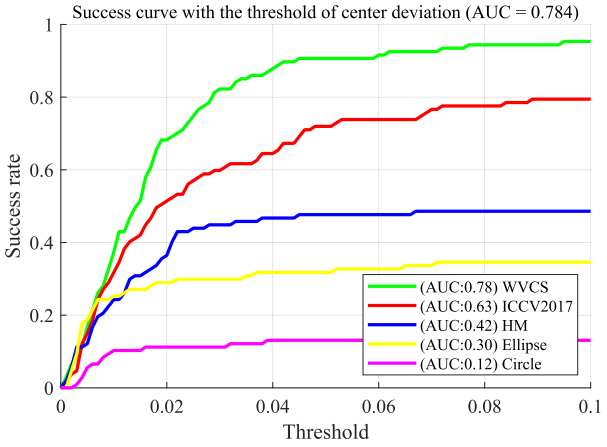

FIGURE 5. Comparison on success rate concerning the ratio between the variation of center and diagonal. The threshold range is [0, 0.1]. When the threshold is beyond 0.1, the distance between the detected center and real center is more than one-tenth of the diagonal, we consider the detection results is wrong. The average success rate is shown in the legend. Best view in color.

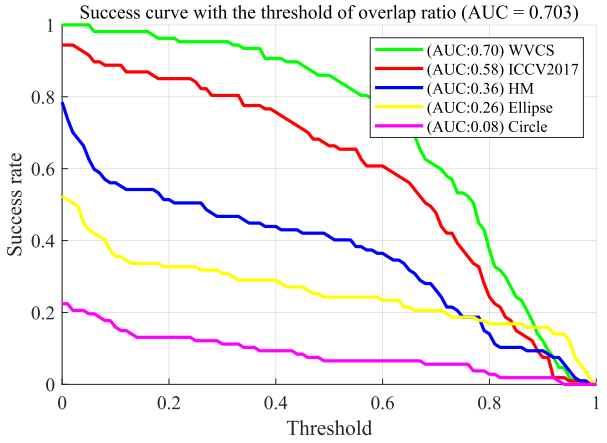

FIGURE 6. Comparison on success rate with overlap ratio. The threshold range is [0, 1]. We can observe that the results are similar to the variation of center distance. The average success rate is shown in the legend. The WVCS outperforms other comparison methods. Best view in color.

the background and the foreground in a similar case, which is equivalent without penalty case. Furthermore, the WVCS can detect the symmetry center when the target object with different colors and defective areas, as shown in the fifth row. And the weight maps Fig. 7(b), Fig. 7(c) and Fig. 7(d) illustrate that the weight map of the WVCS optimizes better than others.

2) OBJECT DETECTION

This method can not only be used for detecting the center of the symmetrical object, but also be used for detecting the bounding rectangle, which indicates the position and size of the object. The object detection results are shown in Fig. 6. These results are similar to symmetrical center detection, in which the performance of the WVCS performs better than other comparison methods. Furthermore, when the threshold is more than 0.9, the eclipse detection method is superior to others including the WVCS. Because the eclipse detection

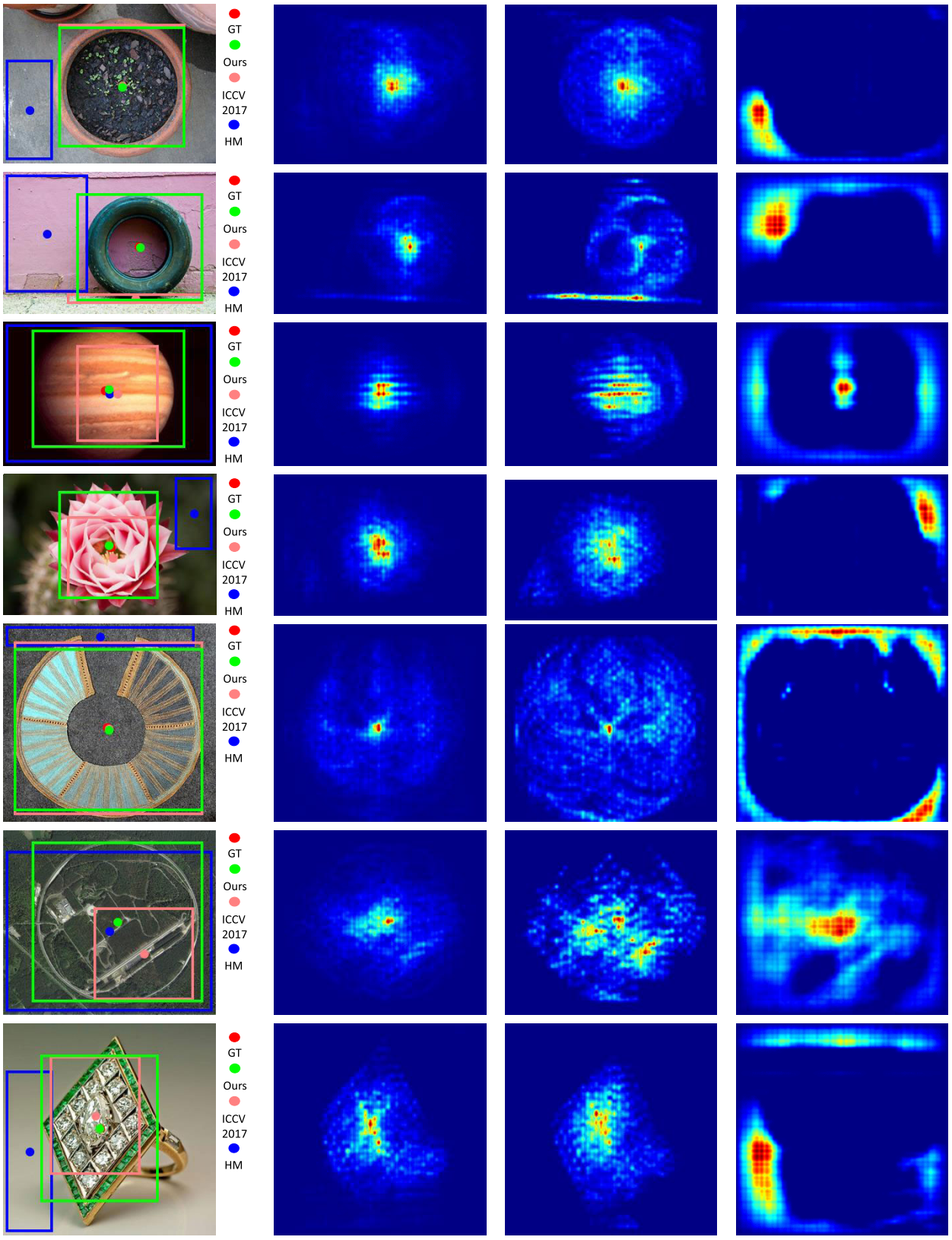

FIGURE 7. Visualization results. (a) The comparative results. Rectangle illustrate the symmetrical object, and it's center is show by the circle point. (b), (c) and (d) The weight maps of proposed method, ICCV2017 and HM, respectively. We can observe that the weight map of WVCS drops sharply when the point gets away from the symmetrical center.

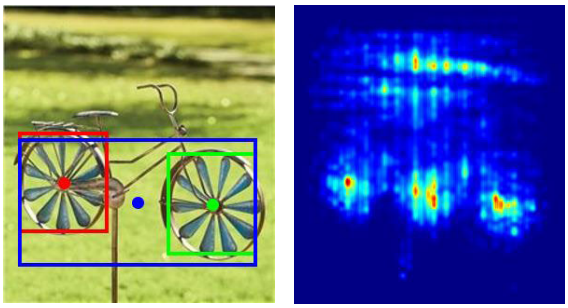

(a) (b)

FIGURE 8. Result of multi-object case. (a) The top three results are shown in order by red, green, and blue. The center of symmetry and the detection result is illustrated by the dot and the rectangle, respectively. (b) The weight map of the symmetrical center point.

method detects the object very well for some clearly elliptical objects. However, the patch-based methods (our method, ICCV2017, and HM) is superior to the eclipse detection method from an overall evaluation. Besides, the performance of ICCV2017 is better than the HM and inferior to our method. Moreover, Fig. 7 illustrates that the WVCS is able to handle various center-symmetrical shapes. This is because our method is based on small patch pairs. The visualization results of the examples are shown in Fig. 7. It can be observed that our method is significantly better than the other methods.

F. MULTI-OBJECT CASE

In some cases, an image may include multiple symmetrical objects. An example is shown in Fig. 8(a), where two tires of the bicycle-shaped windmill are the symmetrical objects. In addition, two tires also form a new symmetrical object. Fig. 8 shows the symmetrical center extraction and object detection results with three local maximums of weight voting. The non-maximum suppression (NMS) is utilized to detect the value of the local maximum. We can find that the top three objects are detected very well in symmetrical centers and object rectangles. This example illustrates that WVCS can also deal with multi-object cases.

V. CONCLUSION

In this article, we propose a novel method for detecting the global symmetry center and the object from an image using a weight voting method. Firstly, we sampled two parts of feature points for voting processing. One is the spatial sampling point, another is the feature point around the edge position. Then, the color information of HSV and the orientation of Log-Gabor response are utilized as the feature descriptor to compute a similarity measure for two feature points. In the similarity measure, a penalty term is utilized to reduce the influence of background parts, which makes the proposed method preferentially focus on the center-symmetrical objects in the foreground. All feature point pairs vote for the position with the maximal weight that is the symmetrical center. With the localized symmetrical center, the center-symmetrical object can be detected by fitting the center-symmetrical point pairs. The experimental results have shown that the WVCS outperforms ICCV2017 by 0.15 for symmetrical center localization. The symmetrical object detection also achieved a satisfactory result, the WVCS outperforms ICCV2017 by 0.12.

The remained future work is to employ center-symmetrical characteristics for color gradient object segmentation in real-world images. Moreover, how many targets are included in a target image is still determined manually, which will be solved in our future work.

REFERENCES

[1] C.-K. Chiu and A. P. Schnyder, "Classification of reflection-symmetry-protected topological semimetals and nodal superconductors," *Phys. Rev. B, Condens. Matter*, vol. 90, no. 20, Nov. 2014, Art. no. 205136.
[2] F. Nunziata, M. Migliaccio, and C. E. Brown, "Reflection symmetry for polarimetric observation of man-made metallic targets at sea," *IEEE J. Ocean. Eng.*, vol. 37, no. 3, pp. 384–394, Jul. 2012.
[3] C.-H. Liu, H. Jiang, and S. Chen, "Topological classification of non-hermitian systems with reflection symmetry," *Phys. Rev. B, Condens. Matter*, vol. 99, no. 12, Mar. 2019, Art. no. 125103.
[4] A. Majumder and S. Changder, "A novel approach for text steganography: Generating text summary using reflection symmetry," *Procedia Technol.*, vol. 10, pp. 112–120, 2013.
[5] I. R. Atadjanov and S. Lee, "Reflection symmetry detection via appearance of structure descriptor," in *Proc. Eur. Conf. Comput. Vis. (ECCV*. Boston, MA, USA: Springer, 2016, pp. 3–18.
[6] I. Atadjanov and S. Lee, "Bilateral symmetry detection based on scale invariant structure feature," in *Proc. IEEE Int. Conf. Image Process. (ICIP)*, Quebec, QC, Canada, Sep. 2015, pp. 3447–3451.
[7] J. Redmon, S. Divvala, R. Girshick, and A. Farhadi, "You only look once: Unified, real-time object detection," in *Proc. IEEE Conf. Comput. Vis. Pattern Recognit. (CVPR)*, Las Vegas, NV, USA, Jun. 2016, pp. 779–788.
[8] R. Girshick, "Fast R-CNN," in *Proc. IEEE Int. Conf. Comput. Vis. (ICCV)*, Boston, MA, USA, Dec. 2015, pp. 1440–1448.
[9] K. He, G. Gkioxari, P. Dollár, and R. Girshick, "Mask R-CNN," in *Proc. IEEE Int. Conf. Comput. Vis. (CVPR)*, Honolulu, HI, USA, Oct. 2017, pp. 2961–2969.
[10] S. Lee and Y. Liu, "Skewed rotation symmetry group detection," *IEEE Trans. Pattern Anal. Mach. Intell.*, vol. 32, no. 9, pp. 1659–1672, Sep. 2010.
[11] G. Loy and J.-O. Eklundh, "Detecting symmetry and symmetric constellations of features," in *Proc. Eur. Conf. Comput. Vis. (ECCV)*. Graz, Austria: Springer, 2006, pp. 508–521.
[12] D. G. Lowe, "Distinctive image features from scale-invariant keypoints," *Int. J. Comput. Vis.*, vol. 60, no. 2, pp. 91–110, Nov. 2004.
[13] Q. Mo and B. Draper, "Detecting bilateral symmetry with feature mirroring," in *Proc. IEEE Int. Conf. Comput. Vis. Workshops (CVPRW)*, Colorado Springs, CO, USA, Mar. 2011, pp. 1–8.
[14] L. Leng, J. Zhang, M. K. Khan, X. Chen, and K. Alghathbar, "Dynamic weighted discrimination power analysis: A novel approach for face and palmprint recognition in DCT domain," *Int. J. Phys. Sci.*, vol. 5, no. 17, pp. 2543–2554, Dec. 2010.
[15] L. Leng, M. Li, C. Kim, and X. Bi, "Dual-source discrimination power analysis for multi-instance contactless palmprint recognition," *Multimedia Tools Appl.*, vol. 76, no. 1, pp. 333–354, Jan. 2017.
[16] D. J. Field, "Relations between the statistics of natural images and the response properties of cortical cells," *J. Opt. Soc. Amer. A, Opt. Image Sci.*, vol. 4, no. 12, pp. 2379–2394, 1987.
[17] D. Gabor, "Theory of communication. Part 1: The analysis of information," *J. Inst. Electr. Eng.-III: Radio Commun. Eng.*, vol. 93, no. 26, pp. 429–441, Nov. 1946.
[18] W. Wang, J. Li, F. Huang, and H. Feng, "Design and implementation of log-Gabor filter in fingerprint image enhancement," *Pattern Recognit. Lett.*, vol. 29, no. 3, pp. 301–308, Feb. 2008.
[19] J. Li, N. Sang, and C. Gao, "Log-Gabor weber descriptor for face recognition," *J. Electron. Imag.*, vol. 24, no. 5, Sep. 2015, Art. no. 053014.
[20] E. Walia and V. Verma, "Boosting local texture descriptors with log-Gabor filters response for improved image retrieval," *Int. J. Multimedia Inf. Retr.*, vol. 5, no. 3, pp. 173–184, Sep. 2016.

[21] C. Mancas-Thillou and B. Gosselin, "Character Segmentation-by-Recognition using log-Gabor filters," in *Proc. 18th Int. Conf. Pattern Recognit. (ICPR)*, Hong Kong, 2006, pp. 901–904.
[22] K. Briechle and U. D. Hanebeck, "Template matching using fast normalized cross correlation," *Proc. SPIE*, vol. 4387, pp. 95–102, Mar. 2001.
[23] J.-C. Yoo and T. H. Han, "Fast normalized cross-correlation," *Circuits, Syst. Signal Process.*, vol. 28, no. 6, p. 819, 2009.
[24] A. Ghosh, B. N. Subudhi, and S. Ghosh, "Object detection from videos captured by moving camera by fuzzy edge incorporated Markov random field and local histogram matching," *IEEE Trans. Circuits Syst. Video Technol.*, vol. 22, no. 8, pp. 1127–1135, Aug. 2012.
[25] M. Mehta, C. Goyal, M. C. Srivastava, and R. C. Jain, "Real time object detection and tracking: Histogram matching and Kalman filter approach," in *Proc. 2nd Int. Conf. Comput. Autom. Eng. (ICCAE)*, Singapore, Feb. 2010, pp. 796–801.
[26] H. Zhang, W. Gao, X. Chen, and D. Zhao, "Object detection using spatial histogram features," *Image Vis. Comput.*, vol. 24, no. 4, pp. 327–341, Apr. 2006.
[27] M. Elawady, C. Ducottet, O. Alata, C. Barat, and P. Colantoni, "Wavelet-based reflection symmetry detection via textural and color histograms: Algorithm and results," in *Proc. IEEE Int. Conf. Comput. Vis. Workshops (ICCVW)*, Honolulu, HI, USA, Oct. 2017, pp. 1734–1738.
[28] S. Tsogkas and I. Kokkinos, "Learning-based symmetry detection in natural images," in *Proc. Eur. Conf. Comput. Vis. (ECCV)*. Florence, Italy: Springer, 2012, pp. 41–54.
[29] R. Kat, R. Jevnisek, and S. Avidan, "Matching pixels using co-occurrence statistics," in *Proc. IEEE/CVF Conf. Comput. Vis. Pattern Recognit.*, Salt Lake City, UT, USA, Jun. 2018, pp. 1751–1759.
[30] E. R. Davies, *Machine Vision: Theory, Algorithms, Practicalities*. Amsterdam, The Netherlands: Elsevier, 2004.
[31] C. Lu, S. Xia, M. Shao, and Y. Fu, "Arc-support line segments revisited: An efficient high-quality ellipse detection," *IEEE Trans. Image Process.*, vol. 29, pp. 768–781, 2020.
[32] P. Pérez, C. Hue, J. Vermaak, and M. Gangnet, "Color-based probabilistic tracking," in *Proc. Eur. Conf. Comput. Vis. (ECCV)*. Copenhagen, Denmark: Springer, 2002, pp. 661–675.
[33] A. A. Rad, K. Faez, and N. Qaragozlou, "Fast circle detection using gradient pair vectors," in *Proc. Dicta*, Sydney, NSW, Australia, 2003, pp. 879–888.

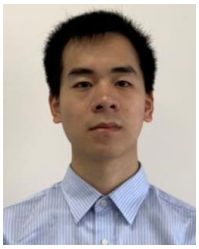

YI ZHANG (Member, IEEE) received the B.E. degree in the computer science and technology from Northwest A&F University, in 2015, and the M.E. degree from Iwate University. He is currently pursuing the Ph.D. degree with the Graduate School of Engineering, Department of Design and Media Technology, Iwate University. His research interests include evolutionary algorithms, image processing, and machine learning.

MIN ZOU received the bachelor's degree from Qufu Normal University, China, in 2012, and the master's degree from Iwate University, in 2015. She is currently pursuing the Ph.D. degree with the Department of Design and Media Technology, Graduate School of Science and Engineering, Iwate University. Her research interests include image processing, deep learning, and machine learning.

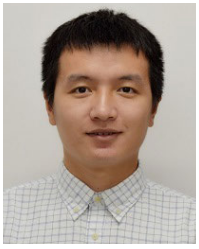

MENGBO YOU (Member, IEEE) received the bachelor's degree from the College of Information Engineering, Northwest A&F University, in 2012, and the master's and Ph.D. degrees from Iwate University, in 2015 and 2018, respectively. He is currently a Lecturer with the College of Information Engineering, Northwest A&F University. His research interests include pattern recognition, machine learning, image processing, object detection, and classification.

TAKUYA AKASHI (Member, IEEE) received the Ph.D. degree in system design engineering from the University of Tokushima, in 2006. Since April 2009, he has been with the Department of Electrical Engineering, Electronics and Computer Science, Iwate University. In 2015, he was a Visiting Associate with the California Institute of Technology. He is currently an Associate Professor with the Iwate University. His research interests include evolutionary algorithms, image processing, and human sensing. He is a member of RISP, IEICE, and IEEJ.